

# Focusing and Steering for Medical Applications with Magnetic Near-Field Arrays and Metasurfaces

Alon Ludwig, Joseph P. S. Wong, Ariel Epstein, Alex M. H. Wong, George V. Eleftheriades, Costas D. Sarris  
 Department of Electrical and Computer Engineering, University of Toronto, Toronto, ON, M5S 3G4, Canada,  
 alon.ludwig@utoronto.ca

**Abstract**—Two recently suggested 2D structures for control of electromagnetic beams are presented; the magnetic near-field antenna array and the Huygens metasurface. Opportunities and challenges in the context of medical applications are discussed.

**Index Terms**—near-field antenna arrays, beam-steering, focusing, Huygens metasurfaces.

## I. INTRODUCTION

The use of the Huygens principle to design active and passive electrically thin surfaces has gained significant attention in recent years [1]. One such structure is the near-field antenna array that forms a low-profile alternative to the bulky subwavelength focusing lens and is designed to produce and control a subwavelength beam on an image plane located in the near-field [2]. Choosing the array elements as capacitively loaded loops, it is possible to achieve a two-dimensionally steerable magnetic-field subwavelength beam with reduced residual surrounding electric-field on a near-field image plane [3]. This property may prove useful in various biomedical applications such as hyperthermia and imaging. Another type of a two-dimensional (2D) structure considered here for similar applications is the Huygens metasurface [4], [5], composed of electric and magnetic polarizable subwavelength elements. In these structures, wavefront control is achieved by the induced electric and magnetic surface currents, enabling focusing and steering of electromagnetic beams. In the following sections those two configurations are described in more detail, with respect to focusing applications suitable for modern biomedical procedures.

## II. MAGNETIC NEAR-FIELD ANTENNA ARRAYS

To create and control subwavelength featured magnetic fields, the proposed array elements are chosen as loops of subwavelength dimensions. The loops are arranged as a 2D coplanar array placed in free-space at a distance  $D_{ip}$  from the image plane (see Fig. 1a). To allow better control over the operation of the loops, they are designed to resonate in the vicinity of the desired operation frequency,  $f_{op}$ . To that end, the loops are implemented as four separate conductor lines creating a rectangle with overlapping regions at the corners, acting as capacitive loads (see Fig. 1b); the overlap can be tuned in size to control the resonant frequency. The device operation is exemplified at a frequency of  $f_{op} = 2$  GHz ( $\lambda_{op} = 15$  cm), allowing one to place the image plane as far as

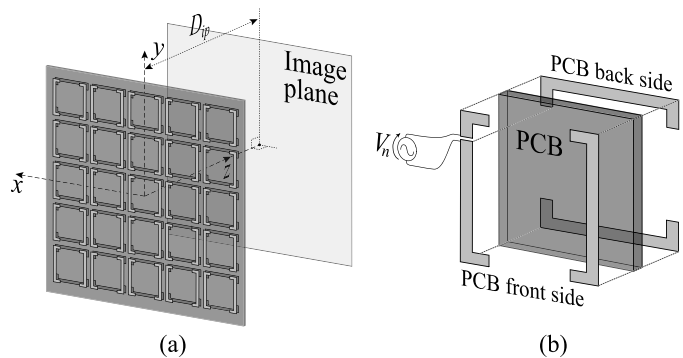


Fig. 1. Loop antenna array geometry. Panel (a) shows the entire array, and panel (b) shows the loop element structure.

$\lambda_{op}/4 = 3.75$  cm from the array. The loop size is  $1\text{ cm} \times 1\text{ cm}$  to allow comparable beam resolution on the image plane.

Excitation of each loop element using a voltage source of a given amplitude and phase, obtained by using the spatially shifted beam approach [2], results in a subwavelength magnetic-field beam on the image plane with a full width half maximum (FWHM) contour of  $0.15\lambda_{op}$  in diameter (see red curve in Fig. 2a)). Interestingly, as the focused magnetic-field

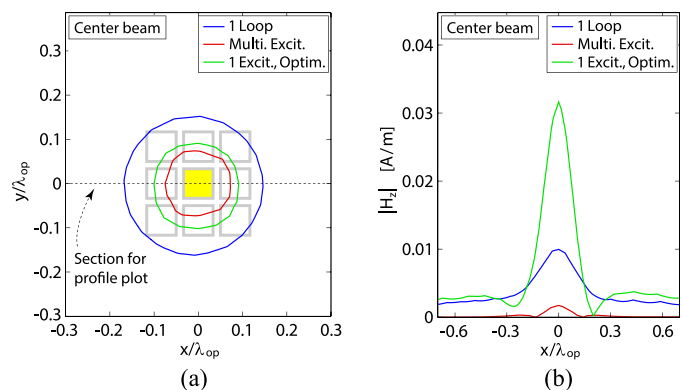


Fig. 2. Comparison of resulting beam for focusing obtained using single element excitation, multiple element excitation, and capacitor-optimized single element excitation. Panel (a) shows FWHM beamwidth contours of the beams, while panel (b) shows the profile of the magnetic field magnitude.

beam becomes narrower, the electric field on the image plane becomes further suppressed. This important result will be further discussed in the context of medical applications. Compared to the single element excitation (blue curve in Fig. 2a),

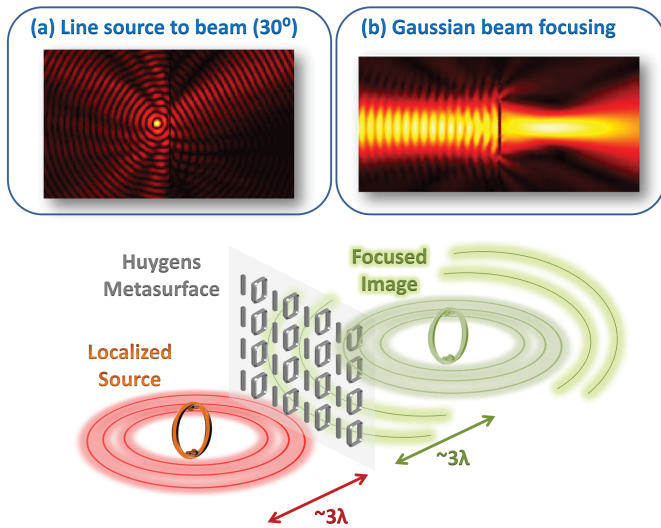


Fig. 3. Illustration of focusing using Huygens metasurface. Insets: HFSS simulated fields of passive HMS (a) converting electric line source fields into  $30^\circ$  directive beam [6]; (b) focusing a Gaussian beam [7].

the focused beam width is significantly narrower; however, its magnetic-field intensity is also significantly smaller. This is a simple outcome of the strong field cancellation due to opposing currents on neighboring elements that is characteristic to all subwavelength focusing arrays.

The reduced focused beam intensity together with the drawback of requiring a complicated feeding network to excite each array element motivated us to study more closely the interaction between loop elements in the array. It was found that such a study can be performed using a simple circuit model that accounts for the mutual inductance between the loops and the radiation resistance. Based on this circuit model, some general underlying properties of the array can be inferred, including the existence of a strong resonance that is characterized by opposing currents on neighboring loops. This inherent opposing-currents resonance is used to initialize an optimization procedure that tunes the array to maximize the achievable magnetic-field intensity of the focused beam while eliminating the need for multiple excitation sources. The tuning is done by introducing lumped capacitors in shunt to one of the loop corners. The green curves in Fig. 2 show the results for the capacitively-tuned optimized array when only the middle loop is excited. It is evident from those plots that a narrow beamwidth can be retained in this single-excitation scenario, while the focused beam intensity is substantially increased.

### III. HUYGENS METASURFACES

An alternative scheme for achieving efficient delivery of electromagnetic power to a limited region within a distant body is based on Huygens metasurfaces (HMS) [4], [5]. This novel class of thin metamaterial slabs builds on the idea that distributed electric and magnetic surface currents can implement an arbitrary discontinuity in the tangential fields,

in accordance with the equivalence principle. The required surface currents can be realized by active elements, directly generating the required current distribution, or by passive polarizable particles, which induce the desirable surface currents in response to a designated excitation. Besides the efficient design approach offered by this concept, effectively employing impedance boundary conditions [1], the collocated electric and magnetic currents may be engineered to promote unidirectional radiation, acting as Huygens sources. Thus, HMSs are attractive since they provide a way to achieve a highly controlled transmitted wavefront with reduced reflections.

We suggest using a Huygens metasurface to convert the fields from a localized source into a focused beam (Fig. 3). Although most reports to date have concentrated on Huygens metasurfaces excited by incident plane-waves or beams [4], [5], we have recently proposed a procedure to integrate localized sources and HMSs to form directive radiation to a desirable angle [6]. By enforcing power conservation and impedance equalization *locally*, we have prescribed a passive lossless design to convert fields from an electric line source one  $\lambda$  away from the HMS to a beam directed at  $30^\circ$  (Fig. 3a). To achieve localization of the transmitted power on the target as well, focusing capabilities must be implemented. We have demonstrated such capabilities in [7], where a passive HMS was designed to focus an incoming Gaussian beam to a spot positioned  $2.78\lambda$  away from the metasurface, with a waist width of  $0.73\lambda$  at the focal point (Fig 3b).

Recently, we have presented a Floquet-Bloch analysis of refracting Huygens metasurfaces, which facilitates ray-oriented design of such structures. Harnessing the results presented in [8], the refraction of an HMS can be tailored locally, allowing synthesis of a lens-like metasurface with finite focal lengths. As depicted in Fig. 3, this enables focusing of a localized source to a diffraction-limited spot, provided the source and image are sufficiently separated from the HMS; implemented with a Huygens metasurface, this focusing can be achieved with little reflections [4], [5]. In addition, ray-optical rationale implies that the focus position inside the target body could potentially be controlled by moving the source position in the focal plane, offering a simple way to achieve scanning capabilities.

Beyond the applications discussed above, the wavefront manipulation capabilities of Huygens metasurfaces can also be facilitated to generate spatial superoscillation wavefronts, which may provide new possibilities for in-body medical imaging, amongst other applications. Fig. 4 shows a 2D full-wave simulation result of a sub-wavelength focused superoscillatory electromagnetic waveform [9]. A superoscillation wave is a collection of propagating waves that interfere to achieve subwavelength variations across a limited interval. Through this phenomenon one can form an electromagnetic waveform with subwavelength (or super-resolution) features at multiple wavelengths away from the excitation surface [10]. This range of working distance is more than an order of magnitude improved from evanescent-wave-based devices, such as the sub-wavelength near-field array introduced in the

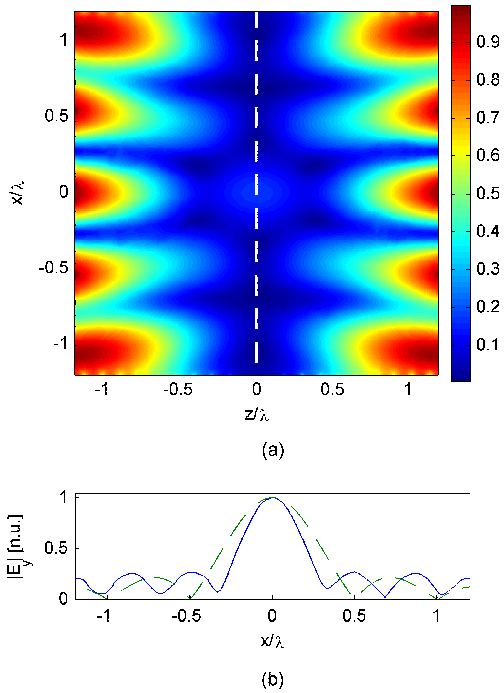


Fig. 4. Superoscillation subwavelength focusing using Huygens metasurfaces. (a) A 2D plot of the electric field distribution within the cavity. Huygens metasurfaces are located across the four boundaries of the cavity; the fields are identically zero outside the cavity. The dashed line denotes the image plane  $z = 0$ . (b) The electric field profile along the image plane (blue, solid), the subwavelength focal width is 70% the width of the diffraction-limited curve (green, dashed).

previous section. In the example shown in Fig. 4, Huygens metasurfaces are placed on all four sides of this environment to excite the propagation waves required to synthesize the waveform. The excitation cavity has a side length of 2.4 wavelengths, hence the image plane in the middle of the cavity stands 1.2 wavelengths separated from the cavity walls. A sub-wavelength electric field focus of dimension  $0.42\lambda$  (full-width at half maximum) is formed along the  $x$ -direction on the plane  $z = 0$ . More aggressive waveform design will lead to sharper focusing and larger separations from the side walls. Notably, the waveform also features a focus along the longitudinal ( $z$ ) direction. This presents a distinctive advantage for superoscillatory focusing in comparison to evanescent-wave-based focusing, for which the electric and/or magnetic field decays exponentially from the source to the image plane. While Fig. 4 shows an electric field focus in a 2D environment, the demonstrated principle can be readily applied to focus magnetic waves in a 3D environment, which may prove more applicable to in-body medical imaging.

#### IV. POTENTIAL IN MEDICAL APPLICATIONS

Both structure types described above have many potential medical applications. The ability of the near-field antenna array to produce narrow and steerable magnetic beams with low residual electric field can be used in medical imaging and therapy applications where high spatial magnetic-field

resolution and a low direct interaction with biological tissue, facilitated by the reduced electric field, is desirable. One possible example is the creation of highly localized magnetic sources for excitation and manipulation of magnetic nanoparticles for hyperthermia, imaging, and drug delivery. Since biological tissue is essentially nonmagnetic, direct interaction with the magnetic fields is minimal and, due to the reduced residual electric field of the array, the interaction will be almost entirely mediated by the magnetic particles. This property is crucial for the accuracy and safety of the prospective imaging and hyperthermia device. Due to relaxation times in the magnetization dynamics of the nanoparticles, the optimal frequency of the external fields is at the low MHz range and the array suggested above should be altered appropriately. The attractive properties of the near-field array discussed above stem from the manipulation of evanescent fields in the vicinity of the array. Those fields are exponentially increasing when moving from the focal plane towards the array, which makes it difficult to achieve localization in the dimension perpendicular to the focal plane.

This shortcoming is not manifested in the aforementioned Huygens metasurface structures, as they are not predominantly based on evanescent fields and, thus, allow focusing in 3D. The first three metasurface structures that were suggested are passive designs demonstrating that it is feasible to harness a localized power source to selectively excite areas at a distance, possibly with scanning abilities. In the case of the metasurface design that maps a source to a focal spot, while the spot is not subwavelength, it is also not restricted to operate in the near-field of the metasurface and therefore allows deeper reach compared with the near-field array. The last example for the use of metasurfaces to achieve focal spots demonstrated the creation of a focused superoscillatory waveform that is both subwavelength and deeply localized. All the structures studied in this paper were placed in free-space and while their operation in the proximity of biological tissue is conceptually possible, it requires additional study. Other topics that may prove important for medical implementation are scaling to frequencies used in medical applications and sensitivity to background and antenna variation.

#### V. CONCLUSION

Two planar structures for focusing and steering electromagnetic beams are discussed. First, near-field antenna arrays are shown to produce narrow and steerable magnetic beams with low residual electric field. The second planar structure discussed is the Huygens metasurface that allows versatile manipulation of target fields at a significant distance. The possible potential those structures have in medical applications was discussed.

#### REFERENCES

- [1] C. L. Holloway, E. F. Kuester, J. a. Gordon, J. O'Hara, J. Booth, and D. R. Smith, "An overview of the theory and applications of metasurfaces: the two-dimensional equivalents of metamaterials," *IEEE Antennas Propag. Mag.*, vol. 54, no. 2, pp. 10–35, Apr. 2012.

- [2] L. Markley and G. V. Eleftheriades, "Meta-screens and near-field antenna-arrays: A new perspective on subwavelength focusing and imaging," *Metamaterials*, vol. 5, no. 2-3, pp. 97–106, Mar 2011.
- [3] A. Ludwig, C. D. Sarris, and G. V. Eleftheriades, "Near-field antenna arrays for steerable sub-wavelength magnetic-field beams," *IEEE Trans. Antennas Propag.*, vol. 62, no. 7, pp. 3543–3556, July 2014.
- [4] C. Pfeiffer and A. Grbic, "Metamaterial Huygens surfaces: tailoring wave fronts with reflectionless sheets," *Phys. Rev. Lett.*, vol. 110, no. 19, p. 197401, May 2013.
- [5] M. Selvanayagam and G. V. Eleftheriades, "Discontinuous electromagnetic fields using orthogonal electric and magnetic currents for wavefront manipulation," *Opt. Express*, vol. 21, no. 12, pp. 14 409–14 429, June 2013.
- [6] A. Epstein and G. V. Eleftheriades, "Passive lossless Huygens metasurfaces for conversion of arbitrary source field to directive radiation," *IEEE Trans. Antennas Propag.*, vol. 62, no. 11, pp. 5680–5695, November 2014.
- [7] J. P. S. Wong, M. Selvanayagam, and G. V. Eleftheriades, "Design of unit cells and demonstration of methods for synthesizing Huygens metasurfaces," *Photonics Nanostruct.*, vol. 12, no. 4, pp. 360 – 375, August 2014.
- [8] A. Epstein and G. V. Eleftheriades, "Floquet-Bloch analysis of refracting Huygens metasurfaces," *Phys. Rev. B.*, vol. 90, no. 23, p. 235127, December 2014.
- [9] A. M. H. Wong and G. V. Eleftheriades, "Superoscillations without sidebands: power-efficient sub-diffraction imaging with propagating waves," accepted for publication in *Sci. Rep.*, January 2015.
- [10] —, "Sub-wavelength focusing at the multi-wavelength range using superoscillations: an experimental demonstration," *IEEE Trans. Antennas Propag.*, vol. 59, no. 12, pp. 4766–4776, December 2011.